Analysis and Correction of Digital Elevation Models for Plain Areas

Cristian Guevara Ochoa, Luis Vives, Erik Zimmermann, Ignacio Masson, Luisa Fajardo, and Carlos Scioli

Abstract

Water movement modeling in plain areas requires digital elevation models (DEMs) adequately representing the morphological and geomorphological land patterns including the presence of civil structures that could affect water flow patterns. This has a direct effect on water accumulation and water flow direction. The objectives of this work were to analyze, compare and improve DEMs so surface water movement in plain areas could be predicted. In order to do that, we evaluated the accuracy of a digital elevation data set consisting in 4064 points measured with a differential global positioning system (GPS) in a plain area of central Buenos Aires province. Three DEMs were analyzed: (1) the Advanced Spaceborne Thermal Emission and Reflection Radiometer (ASTER), (2) the Shuttle Radar Topography Mission (SRTM) and (3) the Advanced Land Observing Satellite with the Phased Array Type L-Band Synthetic Aperture Radar (ALOS PALSAR). Several topographic attributes (i.e., height, surface area, land slope, delimitation of geomorphological units, civil structures, basin boundaries and streams network) and different interpolation methods were analyzed. The results showed that both the SRTM and the ALOS PALSAR DEMs had a ± 4.4 m root mean square error (RMSE) in contrast to the ASTER DEM which had a ± 9 m RMSE. Our analysis proved that the best DEM representing the study area is the SRTM. The most suitable interpolation methods applied to the SRTM were the inverse distance weighting and the ANUDEM, whereas the spline method displayed the lowest vertical accuracy. With the proposed method we obtained a DEM for the study area with a ± 3.2 m RMSE, a 33% error reduction compared to the raw DEM.

Introduction

Earth's surface plays a fundamental role in the modeling of hydrological processes (Wilson and Galán 2000; Wilson 2012; Eric *et al.* 2014). Satellite technologies are currently being developed for capturing topographic information through digital elevation models (DEMs). Through the use of DEMs, geomorphological (Hutchinson *et al.* 2001) and hydrological properties (Jarihani *et al.* 2015) can be analyzed. These include soil moisture (Ludwig and Schneider 2006; Gao *et al.* 2016), flood impact (Sanders 2007; Tarekegn *et al.* 2010; Gichamo *et al.* 2012; Yan *et al.* 2014; Wurl *et al.* 2014), soil stability, potential erosion, precipitation retention, channel shape, land depressions, etc. (Barnes *et al.* 2014).

DEMs have been used for a variety of environmental applications, such as modeling water processes. The most commonly used data for DEMs are radar and radiometric reflection data such as Advanced Spaceborne Thermal Emission and Reflection Radiometer (ASTER) data (Ica and Hook 2002; Pachri *et al.* 2013; Carrascal *et al.* 2013). There are many examples of DEMs using Shuttle Radar Topography Mission (SRTM) data (e.g., Gesch *et al.* 2006; Lin *et al.* 2013; Sharma and Tiwari 2014). Likewise, other applications use Advanced Land Observing Satellite with the Phased Array Type L-Band Synthetic Aperture Radar (ALOS PALSAR) data (e.g., Pontes *et al.* 2017; Hidayat *et al.* 2017).

Currently, the models that quantify surface water movements require a better resolution. Therefore, semi-distributed and distributed models appeared to reproduce various processes that occur in the water balance, such as evaporation, runoff and infiltration. According to Easton *et al.* (2008), Vaze *et al.* (2010), and Guevara (2015), the relief represents an important aspect for which the detailed topography adequately representing the hydrology is needed. This is because when hydrological studies are carried out in plain areas DEMs do not properly represent the hydrological characteristics of the surface (Callow *et al.* 2007).

According to Chaubey *et al.* (2005), the DEM resolution conditions model calibration, having an effect on basin delineation and total surface area (Martz and Jong 1988), drainage network prediction (Chen *et al.* 2012), subcatchment classification and slope.

The relationship between topography and water flow is less clear in plain areas, where low height gradients and depressions make surface flow tracing more complex (Gallant and Dowling 2003). This difficulty is aggravated by the civil structures that contribute to the topographic uncertainty in these areas, since any structure with a height even below 1 m has a significant impact on the surface flow in terms of its direction and quantity (Guevara 2015). On the other hand, the water flow in plain areas does not strictly follow the topography, especially in water excess conditions.

In plain areas, DEMs do not adequately represent the channel geometry. This leads to misinterpretations of the hydraulic factor of water transport, estimated from the

Cristian Guevara Ochoa, Luis Vives, Ignacio Masson, and Luisa Fajardo are with the Instituto de Hidrología de Llanuras "Dr. Eduardo Jorge Usunoff", IHLLA, República de Italia 780 C.C. 47 (B7300) Azul, Buenos Aires, Argentina (cguevara@ihlla.org.ar).

Cristian Guevara Ochoa and Erik Zimmermann are with the Concejo Nacional de Investigaciones Científicas de Argentina, CONICET, Av. Rivadavia 1917, (C1033AAJ) Ciudad Autónoma de Buenos Aires, Argentina.

Erik Zimmermann is with the Centro Universitario Rosario de Investigaciones Hidroambientales, CURIHAM, Riobamba 245 bis (2000) Rosario, Santa Fe, Argentina.

Ignacio Masson and Luisa Fajardo are with the Comisión de Investigaciones Científicas de la provincia de Buenos Aires, CIC, Calle 526 e/10 y 11, La Plata, Buenos Aires, Argentina.

Carlos Scioli is with the Centro de estudios de variabilidad y cambio climático, CEVARCAM, Facultad de Ingeniería y Ciencias Hídricas, Universidad Nacional del Litoral, Paraje el pozo C.C. 217, Ruta Nacional Nº 168, Km 472, Santa Fe, Argentina.

Photogrammetric Engineering & Remote Sensing
Vol. 85, No. 3, March 2019, pp. 11–xxx.
0099-1112/18/11–xxx
© 2019 American Society for Photogrammetry and Remote Sensing
doi: 10.14358/PERS.85.3.xxx

cross-sectional geometry of the channel, which negatively affects water levels, flow rates, time, flood wave velocity and simulated flood dynamics (Tarekegn *et al.* 2010).

Therefore, most of the time it is necessary to correct the DEMs since they generally do not represent the natural and artificial channels, main and secondary roads, and other structures that could be a few meters wide and deep (Scioli 2009; Guevara 2015). These errors could be corrected by adjusting the height of the DEM using multiple sources of information, such as topographic maps, satellite images, interpolation methods and vectors taken by differential global positioning system (GPS) on roads, depressions and channels.

DEMs provide essential spatial data for hydrological and hydrodynamic modeling. For this reason, the resolution of the DEM and the method with which elevation data were interpolated affect the quality of the results.

There is a wide variety of interpolation methods either deterministic (e.g., inverse distance weighting, natural neighbor, spline and ANUDEM) or geostatistical (e.g., kriging). However, there are few published studies on the effectiveness of interpolators applied to the same data set. Most studies were carried out by Reuter *et al.* (2007) and Yang and Hodler (2013). There are different techniques for DEM correction in hydrological modeling. Among them the ANUDEM interpolation stands out as a response to the elimination of data noise (Callow *et al.* 2007). This method interpolates surface data through points, lines and polygons (Hutchinson 1989).

There is no agreement on which are the best methods of interpolation, if deterministic methods or geostatistical methods. Several authors such as Paredes *et al.* (2013) and Yang and Hodler (2013) recommended that DEM validations should be carried out locally to make better decisions as to which interpolation method works best. Some studies establish that geostatistical methods are more reliable for the prediction of height values (Guo *et al.* 2010; Arun 2013), while others, such as Reuter *et al.* (2007), come to a different conclusion suggesting that deterministic methods are better for predicting height values.

The objectives of this study were: (a) To evaluate, by means of using different statistical procedures and graphics, the vertical accuracy of ASTER, SRTM and ALOS PALSAR DEMs in plain areas, accounting for the morphological, geomorphological and civil structures in the terrain, in order to get the best DEM representing topographic variability (b) to compare vertical accuracy using different interpolation methods applied to the best DEM and (c) to establish guidelines for the correction of DEMs in plain areas.

Study Area

The study area was located in the center of the province of Buenos Aires (36.8°–37.3° S, 58.8°–60.1° W). With a surface area of 2,725 km^2 (Figure 1), it covers Del Azul upper creek basin. The main stream origins in the town of Chillar (60 km south of the city of Azul) and its main tributaries are the Videla stream with a 120 km^2 sub-basin and the Santa Catalina stream with a 138 km^2 sub-basin.

The geomorphology of the study area is dominated by positive reliefs in the hills zone (Tandilia system) and decreases towards the north, where there is a depressed zone, with very soft and low reliefs and <1% slopes. This area lacks of a developed drainage system. In periods of water excess this causes the entire surface of the landscape to become flooded due to the low hydraulic capacity of the channels (Guevara 2015).

The study area is characterized by being shaped by the action of wind, due to the low morphometric potential and the fine granulometry of the soils, which makes it prone to wind erosion. The concentrated action of wind deflation in these zones is capable of excavating closed depressions, known as deflation hollows, which play a very important role in the water flow and storage in these areas.

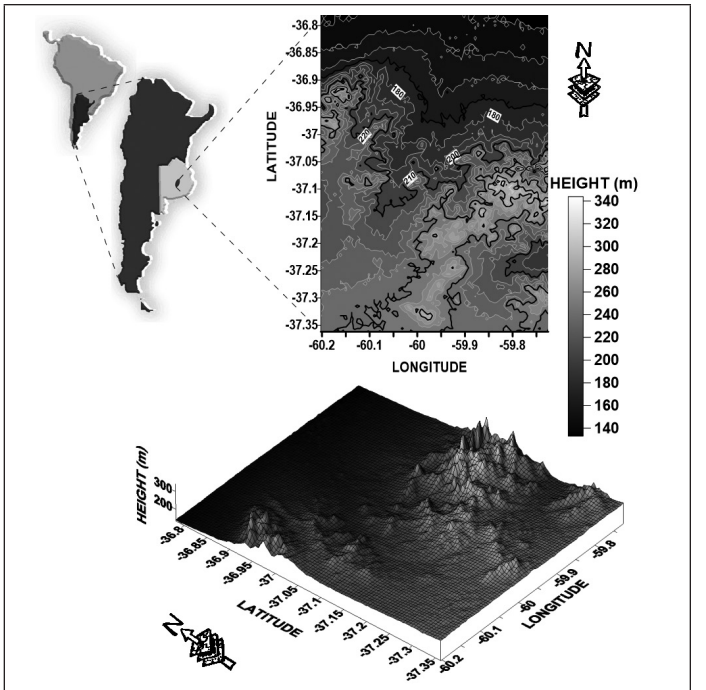

Figure 1. Location and elevation of the study area (2D and 3D view).

The water moves northeast from the Tandilia hills system and it is mainly lost by evaporation (Zabala *et al.* 2015). This is one of the regions of the world with the lowest morphometric potential and for this reason surface runoff has a shallow but extensive coverage. In this landscape, deflation hollows play a very important role in the movement of water, since these are connected forming a runoff pathway parallel to the flow of the main channel.

Methodology

In this section, we present the observed data set we worked with, we describe the used DEMs, we explain how we calculated the flow and accumulation of water for the drainage network, we describe the deterministic and geostatistical interpolation methods we used, and finally, we explain how the accuracy of the DEM was determined.

Data Collection Using a GPS

To evaluate the vertical accuracy of the DEMs, a differential GPS unit was used. This type of GPS measures height using the EGM96 projection (Lemoine *et al.* 1998). This is a datum that takes into account the height of the geoid and through which the vertical accuracy of a DEM could be evaluated.

A Thales Promark 3 differential GPS unit was the particular equipment used for the measurements. This equipment allows the post-processing of the measured points using Global Navigation Satellite System (GNSS) software to correct for vertical errors and bring them down to the cm range. To analyze the vertical accuracy of the DEMs in the study area, eight control points 10 km apart from each other were used and a topographic survey accounting for 4064 points was carried out.

Differential GPS data points were taken on main and secondary roads, land depressions and in the stream channel (bathymetry). Figure 2 shows the location of the GPS measured points and the control points, and some graphic examples of how points were distributed in order to account for the particular topographic features of the study area.

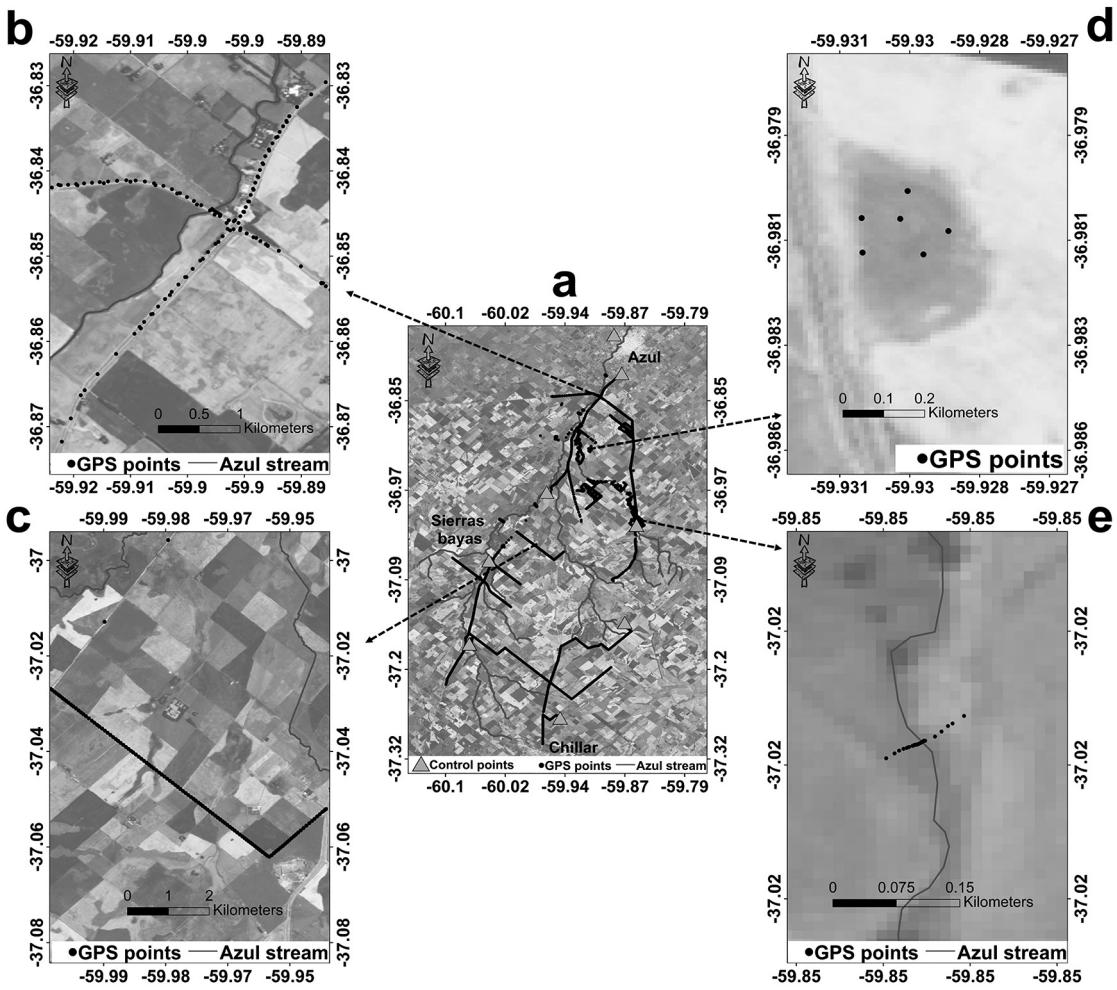

Figure 2. (a) Location of the points measured using differential GPS and the control points for the study area, (b) GPS points measured on main roads, (c) GPS points measured on secondary roads, (d) GPS points measured in a deflation hollow, (e) GPS points measured in the stream channel (bathymetry). Source: satellite image SPOT 5.

Description of the Used DEMs

Advanced Spaceborne Thermal Emission and Reflection Radiometer (ASTER)

This DEM created by the Ministry of Economy, Trade and Industry of Japan (METI), uses an infrared spectral band generating stereo images, with a base-height ratio of 0.6 (Tachikawa *et al.* 2011) that covers the world land surface from 83° N to 83° S (Abrams *et al.* 2015). It has a spatial reference of 1 arc second (~30 m) worldwide coverage. The digital elevation model (GDEM) Version 2 was released in October 2011 (three years after its predecessor, Version 1), along with the addition of 200 000 new images for the stereoscopic process, several anomalies were corrected, and its overall accuracy was improved. This DEM has a ±17 m vertical accuracy (Mukherjee *et al.* 2013; Rexer and Hirt 2014; Robinson *et al.* 2014).

Shuttle Radar Topography Mission (SRTM)

This DEM is a cooperative project between the United States National Aeronautics and Space Administration (NASA) and the United States Department of Defense's National Imagery and Mapping Agency (NIMA). The mission was designed to use a radar interferometer to produce a digital elevation model of the Earth's surface between approximately 60° N and 56° S, that is about 80% of the Earth's land mass (Rabus *et al.* 2003). This mission was carried out for 11 days in February 2000. This DEM has a spatial reference of 1 second of arc (~30 m) and has a ±16 m vertical precision (Sun *et al.* 2003; Kelldorfer *et al.* 2004; Gesch 2006).

Advanced Land Observing Satellite (ALOS PALSAR)

The DEM of the Advanced Land Observing Satellite (ALOS) was created by the Japan Space Exploration Agency (JAXA) and uses the synthetic L-band type aperture sensor (PALSAR) which operates at a band width of 14 to 28 MHz. This DEM has a spatial resolution of 12.5 m and covers an area of 156.25 m^2 per pixel (Kimura and Ito 2000; Rosenqvist *et al.* 2007; Chu and Lindenschmidt 2017). It has a WGS84 horizontal reference datum and the vertical datum is modified by means of the gravitational model of the earth (EGM08) that takes into account the vertical reference of the geoid (Pavlis *et al.* 2012).

Calculation of Drainage Network and Delimitation of the Basin

These tasks were performed using the Archydro extension of ArcGIS (ESRI 2011) for the geographical region corresponding to the Del Azul upper creek basin. The Archydro extension uses the D8 algorithm (Tarboton 1997) with which the water flow in each pixel is evaluated considering its eight neighboring pixels. Once flow directions are calculated, the flow field (i.e., the area contributing to each cell or pixel of the grid) is

quantified to define the resulting direction of the flow and the accumulation of water. This allows the delimitation of the basin boundaries in order to compare the different contributing areas discretized by each DEM.

Interpolation Methods

An element that introduces error into DEMs is the interpolation method used to generate the model. Interpolation methods are procedures used to predict values at locations lacking sampling points. These methods are based on the principle of spatial autocorrelation or spatial dependence (Childs 2004). Previous studies have presented results that do not agree with each other as to the accuracy of the different interpolation methods used for the generation of the DEMs (Wechsler and Kroll 2006; Reuter *et al.* 2007; Yang and Hodler 2013; Arun 2013). In order to contribute to this discussion and to improve our understanding of the error introduced by the interpolation methods in DEMs, our study evaluates and compares the precision of DEMs generated using two different interpolation methods: the deterministic and the geostatistical methods.

Deterministic Methods

Spatial interpolation is a procedure used to calculate the value of a variable in a certain spatial position, knowing the values of that variable in other positions of the space.

Inverse Distance Weighting (IDW)**:** According to (Bartier and Keller 1996), this method uses a higher allocation or gives a higher weight to the nearest point with this weight decreasing as the distance increases, depending on the power coefficient.

$$z_{x,y} = \frac{\sum_{i=1}^{n} z_i w_i}{\sum_{i=1}^{n} w_i} \tag{1}$$

where:

$z_{x,y}$: It is the estimate of the height at the point (x,y).
z_i: It represents the control value for the ith sampling point.
w_i: It is a weight that determines the relative importance of the individual control point Z, in the interpolation procedure.
n: It is the number of points.

The value of the missing data is estimated based on a weighted average of the measured data and a weight is assigned at each point depending on its location. The equation is:

$$w_i = d_{x,y,i}^{-\beta} \tag{2}$$

where:
$d_{x,y,i}$: It is the distance between $z_{x,y}$ and z_i.
β: It is a user-defined exponent, in this case it is 2 because the inverse of the squared distance was used.

Natural neighbor**:** Sibson (1981) developed a weighted average function, called natural neighbor interpolation. This method is based on the Voronoi diagram, applied to a discrete set of spatial points. Natural neighbor interpolation finds a subset of samples closest to an input query point and applies weights to them based on proportional areas to interpolate a value. It is a spatial autocorrelation method, which decreases the standard deviation (STD) of values (Wechsler and Kroll 2006).

This type of interpolation is similar to IDW, it calculates the point value depending on the position of the neighboring point.

$$Z_{x,y} = \sum_{i=1}^{n} w_i Z(s_i) \tag{3}$$

where:
$Z_{x,y}$: It is the estimate of the height at the point (x,y).
w_i: It is a weight that determines the relative importance of point Z.
$Z(s_i)$: It is the measured value at the location $i(x_i, y_i, z_i)$.
n: It is the number of points.

Spline**:** This method calculates the height value at a point, with a mathematical function that minimizes curvature of the surface, resulting in a smoothed surface, which passes exactly through the points in the sample (Childs 2004).

This method uses low-grade polynomials, thus avoiding undesirable fluctuations in most of the applications found, by interpolating using high-grade polynomials (Wahba and Wendelberger 1980). In our study, we used the regularized spline method that incorporates the first derivative of the slope.

The spline interpolation is calculated with the following formula:

$$Z_{(x,y)} = T_{(X;Y)} + \sum_{j=1}^{n} \lambda_i R(r_i) \tag{4}$$

where:
$Z_{(x,y)}$: It is the estimate of the height at a point (x,y).
i: It is the point number.
n: It is the total number of points.
λ_j: It is a coefficient determined by solving a system of linear equations.
r_i: It is the distance from point (x,y) to point i.
$T_{(x,y)}$ and (r): These are defined differently according to the selected option.

The regularized spline interpolation option was the method used in this study. The calculation used $T_{(x,y)}$ and (r) from the following equations:

$$T(x,y) = a1 + a2x + a3y \tag{5}$$

where:
a_i: The coefficients are determined by solving the system of linear equations.

And (r) is determined by the following formula:

$$R(r) = \frac{1}{2\pi}\left\{\frac{r^2}{4}\left[\ln\left(\frac{r}{2\tau}\right) + c - 1\right] + \tau^2\left[K_0\left(\frac{r}{\tau}\right) + c + \ln\left(\frac{r}{2\pi}\right)\right]\right\} \tag{6}$$

where:
r: It is the distance between the point and the sample.
τ: It is the weight of the parameter.
K_0: It is the modified Bessel function.
c: It is a constant equal to 0.577215.

ANUDEM**:** This algorithm was developed by Hutchinson (1989). It constitutes a morphological approach to the interpolation of digital elevation models and uses a specially designed interpolation technique to create a surface that represents more accurately the drainage system.

It is an adaptive mesh that is commonly used for the calculation of digital elevation models in a regular grid. It includes the implementation of the algorithm and the application that imposes a drainage structure connected to an interpolated DEM (Hutchinson *et al.* 2011).

This coupling is performed with an iterative interpolation technique based on finite differences, which optimizes computational efficiency through Childs (2004) minimization.

$$\sum_{i=1}^{n}\left[\frac{z_i - f\left(x_{i,}\ y_i\right)}{w_i}\right]^2 + \Lambda J(f) \tag{7}$$

where:
$J(f)$: It is the roughness of the terrain as a function of the first and second derivative of f.
Λ: It is the positive parameter that softens said roughness.
f: It is an unknown bivariate function representing a finite difference mesh.

Parameter Λ is chosen so that the sum of squares of the residuals in the equation above is equal to n, which can only be achieved by an iterative interpolation method for which, the slope of each cell is available. That is, the ANUDEM method generates a low-resolution DEM and interpolates improving the resolution until reaching the solution.

$$z_i = f(x_i, y_i) + \varepsilon_i (i = 1, \ldots, n) \tag{8}$$

where:
n: It is the number of elevation samples.
ε_i: It is the random error with mean 0 and standard deviation given by:

$$w_i = hs_i\sqrt{12} \tag{9}$$

where:
h: It is the cell size of the mesh.
S_i: It is the slope of the cell associated with the sample.

Geostatistical Method (Kriging)
This method developed by Matheron (1965) is a local spatial interpolation, based on variogram theory and structural analysis (Zhang *et al.* 2015). It is a spatial correlation of the data points measured by the variogram function. The peculiarity of this type of interpolation is that it has the ability to produce a prediction surface but also provides some degree of certainty or accuracy of predictions.

The kriging interpolation method uses the following formula:

$$Z_{(x,y)} = \sum_{i=1}^{n} \lambda_i Z\left(s_i\right) \tag{10}$$

where:
$Z_{(x,y)}$: It is the estimate of the height at a point (x,y).
$Z(s_i)$: It is the measured value at location $i(x_i, y_i, z_i)$.
λ_i: It is an unknown weight n for the measured value at position i.
n: It is the number of measured values.

The method used in our study is ordinary kriging. It is the most general and most widely used kriging method. It assumes the mean is constant and unknown. The variogram model used is spherical, which shows a progressive decrease in the autocorrelation (and in the increase of semivariance) of the distance.

Evaluation of Vertical Accuracy of DEMs

To evaluate the accuracy of the different digital elevation models, Wechsler and Kroll (2006) and Shortridge and Messina (2011) recommended three different types of statistics (root mean square error, coefficient of determination and standard deviation).

According to Wilson and Galán (2000) the most used statistic for the evaluation of digital elevation model's accuracy is the root mean square error (RMSE). The RMSE represents the standard deviation of the differences between the calculated values and the observed values in the sample. These individual differences are known as residuals, when calculations are carried out on the sample data used for the estimation of prediction errors. The RMSE is a suitable measure of accuracy, but only to compare prediction errors for a particular variable and not among variables, since it is scale dependent. The desired RMSE value is 0, indicating that the method did not produce errors.

Another method to evaluate is the use of the coefficient of determination (R^2). It is a statistic that describes the proportion of variance in the observed data. It is the square of the Pearson correlation coefficient, which varies between 0 and 1. When R^2 adopts high values it indicates a smaller variance of the error, in general, values above 0.7 are considered acceptable. The R^2 has been widely used for hydrological evaluation, although it is more sensitive to extreme values.

The standard deviation is a measure of dispersion also used. It is the square root of the variance of the variable, and the deviation is the distribution that presents the data around the arithmetic mean.

Results

The detailed results of the study are presented in the following subsections. We first defined the general differences between the three models at representing elevation, area and slope for the study area. Then we analyzed in a detailed scale the differences of the three models at reflecting the topographic attributes of the terrain such as geoforms, civil structures and stream channel shape (bathymetry). We also examined the direction of the water flow and water accumulation in order to characterize the drainage network and to delineate basin boundaries. Thereafter, the DEM that best represented the topography of our study area was chosen. Finally, in order to improve the accuracy of the chosen model, we examined different interpolation methods.

Differences Among DEMs

Figure 3 shows the height differences among the three DEMs. For the ASTER model, height ranged from 371 to 115 m. For the SRTM model height ranged from 370 to 114 m. And for the ALOS PALSAR model height ranged from 368 to 114 m. When we evaluated the vertical differences among ASTER, SRTM and ALOS PALSAR models for the plain zone, the linear regression analysis we performed revealed a strong significant correlation between the GPS measured height and the height provided by each of the three DEMs. However, this correlation was stronger both for the SRTM and the ALOS PALSAR models (R^2 = 0.98 for both) than for the ASTER model (R^2 = 0.93) (Figure 4). It is interesting to note that in all three cases the slope value of the regression line was close to 1.

Figure 5 shows the boxplot for the GPS and the DEMs data. In this graph we can differentiate the frequency distribution, the symmetry of the data in terms of elevation and its atypical values. The SRTM and ALOS PALSAR DEMs showed a height distribution with a symmetry and a degree of homogeneity comparable with that of the GPS data. Unlike these two DEMs, the ASTER model showed a more asymmetric data distribution when compared to the GPS data distribution as well as more dispersion and atypically higher values.

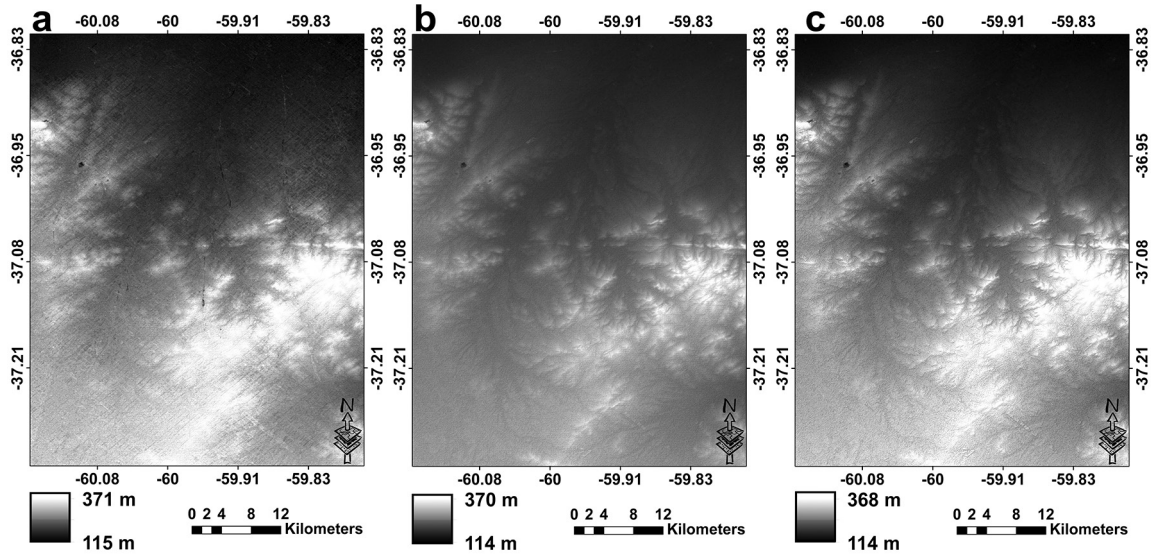

Figure 3. Height differences among the three studied DEMs. (a) The Advanced Spaceborne Thermal Emission and Reflection Radiometer (ASTER GDEM2), (b) The Shuttle Radar Topography Mission (SRTM). Source: Earth explorer, (c) The Advanced Land Observing Satellite (ALOS PALSAR). Source: Alaska satellite facility.

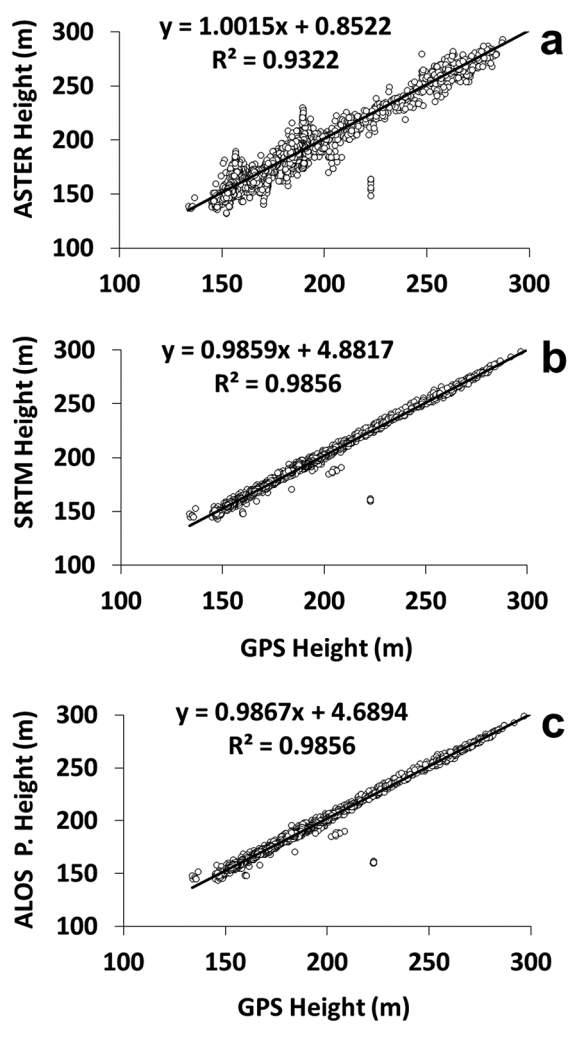

Figure 4. Scatterplots of DEMs heights versus GPS heights. (a) ASTER, (b) SRTM, (c) ALOS PALSAR.

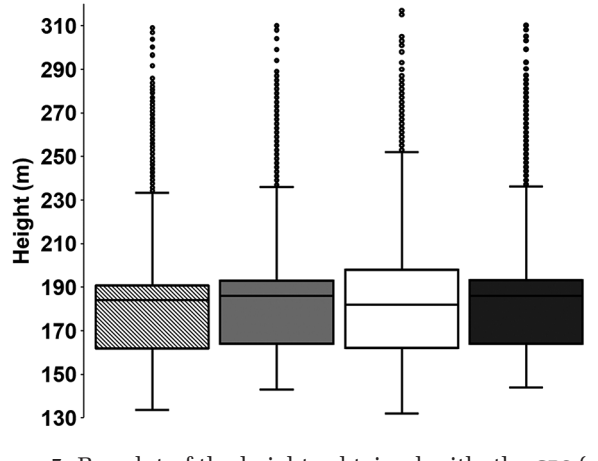

Figure 5. Boxplot of the heights obtained with: the GPS (grey box with diagonal pattern), the SRTM model (solid gray box), the ASTER model (white box), and the ALOS PALSAR model (black box).

Analysis of Topography

The topography of plain zones is one of the main factors affecting DEMs vertical accuracy due to the low morphometric potential of these areas. To evaluate topography, the DEMs were divided into four different elevation bands (<150 m, 150–200 m, 200–250 m, and >250 m) and the slope was analyzed considering two ranges (≤3%, >3%).

Figure 6a shows the obtained areas within each elevation band using the ASTER, the SRTM and the ALOS PALSAR models. The greatest difference was in between the 150–250 m range.

Vertical accuracy regarding the relative area is shown in Figure 6b, which indicates that 10% of the area had <5-m-errors, 40% of the area had 4.5–8.5 m errors, 85% of the area had 3.3–7.7 m errors.

Figure 6c presents the RMSE of the elevation grouped by elevation band for each of the studied DEMs (ASTER, SRTM and ALOS PALSAR). A major error was detected in the three models for the 150–200 m elevation band, thus causing an increase in the uncertainty of the measurements within this height range. A greater error range was found for the ASTER model with a ±5.0–8.5 m RMSE. The RMSE for SRTM was ±2.60–4.5 m whereas for the ALOS PALSAR RMSE was ±2.5–4.5 m. Regarding

the topography representation, SRTM and ALOS PALSAR offered greater precision both in the upper and lower zones compared to ASTER.

In addition, the vertical accuracy among ASTER, SRTM and ALOS PALSAR was evaluated in terms of slope (Figure 6d), showing that the SRTM and the ALOS PALSAR models presented better fit slopes (RMSE ±4.4 m for both) compared to ASTER (RMSE ±9.1 m).

Geomorphological Analysis

The analysis of the geoforms focused on the deflation hollows. Due to the characteristics of the study area they were grouped into two categories, one corresponding to the high zone of the study area with >3%-slopes and another corresponding to the low zone of the study area with <3%-slopes (Figure 7). From the three tested models, the ALOS PALSAR best represented the shape of the deflation hollows. The RMSE for this model was ±1.8 m in the high zone and ±2.3 m in the low zone, with a STD: ±1–1.25 m. The RMSE values for SRTM were ±2.8 and ±3.4 m in the high and low zones, respectively, and a STD: ±1.58–1.8 m. The ASTER model did not delineate correctly the deflation hollows. RMSE values were ±3.4 and ±3.5 m for the high and the low zones, respectively, with STD being ±1.9–2.2 m.

Analysis of DEM Response to the Presence of Civil Structures

Due to the low morphometry of the study area, main and secondary roads are raised onto embankments, so that they can be functional even in periods of water excess. These embankments form a barrier affecting surface flow and lead to a change in the direction and amount of water moving over the surface.

The accuracy of the three DEMs was evaluated in terms of how effectively they represented these structures. As we did for the analysis of the geoforms, the study area was divided into a high and a low zone. We found out that the SRTM model best represented the main and secondary roads as observed in Figure 8. For the main roads, the RMSE for SRTM was ±1.9–6 m (STD: ±4.4–10.7 m) whereas for the ALOS PALSAR and ASTER RMSE values were ±2.3–6.2 m (STD: ±4.6–10.8 m) and ±6.7–12 m (STD: ±5.2–11.8 m), respectively. For the secondary roads the SRTM showed a RMSE of ±2.6 m, whereas for the ALOS PALSAR and ASTER RMSE values were ±2.75 m and ±9.7 m, respectively.

Evaluation of Basin Delimitation and Drainage Network

Basin delimitation and drainage network analysis in the study area were carried out using the Archydro extension of ArcGIS as described in the methods section the location coordinates at the watershed outlet point were -36.83° S and -59.89° W.

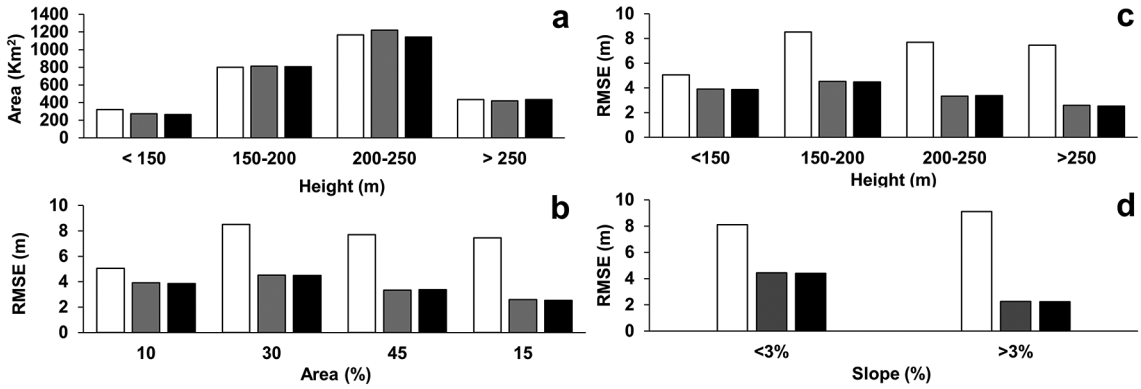

Figure 6. Effect of topography on the vertical accuracy of the digital elevation models. ASTER (white bars), SRTM (gray bars) and ALOS PALSAR (black bars). (a) Distribution of basin surface area (km²) for each tested DEM grouped by elevation band, (b) Relationship between vertical accuracy and relative area for each of the tested DEMs, (c) Relative vertical accuracy of the terrain topography, (d) Relative vertical accuracy of the terrain slope in percent (%).

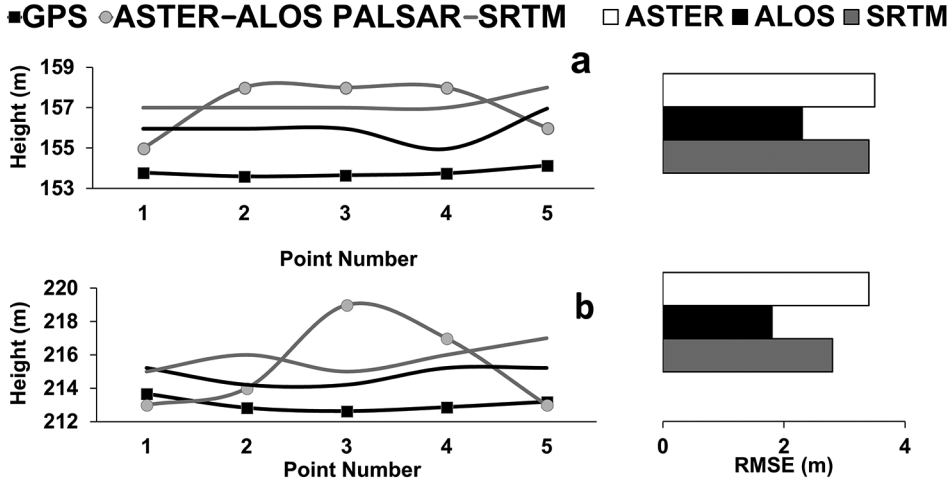

Figure 7. Profile comparison between GPS height measurements and height information from the three tested DEMs (ASTER, SRTM and ALOS PALSAR) at the same location point. (a) Deflation hollow in the low zone of the study area, (b) Deflation hollow in the high zone of the study area.

The drainage network was generated using a treshold surface area of 2100 ha. (i.e., only areas above this treshold value were considered). Basin delimitation was better represented by SRTM and ALOS PALSAR than by ASTER. The former DEMs produced drainage networks which fitted more closely to the drainage network obtained from digitized topographic maps at 1:100 000 scale (Figure 9), both for the upper and lower part of the basin.

The ASTER was the worse of the three DEMs in correctly delimiting the drainage network. This DEM produced inconsistencies especially in for the upper part of the basin (Figure 9). This inconsistences could be attributed to the photogrammetric DEM overestimating the lower order streams as suggested by Thomas and Prasanna Kumar (2015) and Dass and Pardeshi (2018). These errors lead to the obtention of different runoff surfaces areas among DEMs (Table 1), translating into future errors when performing hydrological modeling either for distributed or semi-distributed models, due to the fact that the surface-subsurface flow and concentration time are misestimated.

As for the drainage network, the accuracy of each DEM was analyzed in terms of how well the shape of the stream channel in the plain zone of the basin was represented. The three DEMs had difficulties representing the stream channel in the study area (Figure 10), although the SRTM and ALOS PALSAR models better accounted for the variation in the topography and better resembled the shape of the channel compared to the ASTER model. The following were the RMSE and STD for each of the tested DEMs: SRTM (RMSE: ±2.2–6.8 m, STD: ±1.3–3.6 m), ASTER (RMSE: ±3.3–6.1 m, STD: ±2.3–3.3 m) and ALOS PALSAR (RMSE: ±2.5–6.8 m, STD: ±1.4–3.7 m). These errors were greater in the lower zone of the study area.

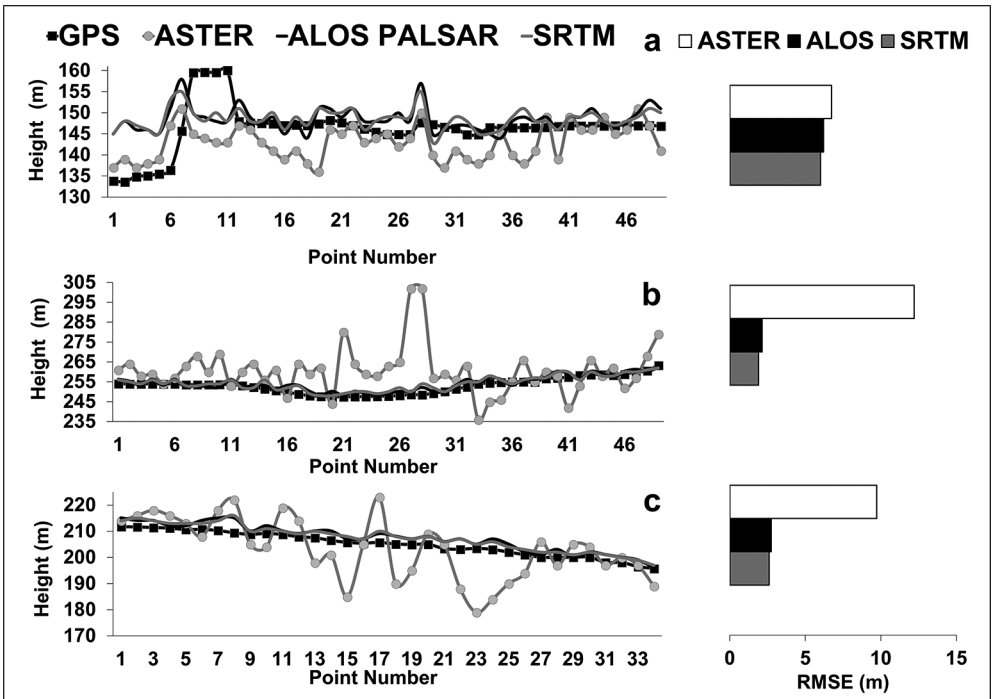

Figure 8. Profile comparison between GPS measured heights and heights provided by each of the three DEMs (ASTER, SRTM and ALOS PALSAR) at locations presenting civil structures. (a) highway at the low zone of the study area, (b) highway at the high zone of the study area, (c) secondary road.

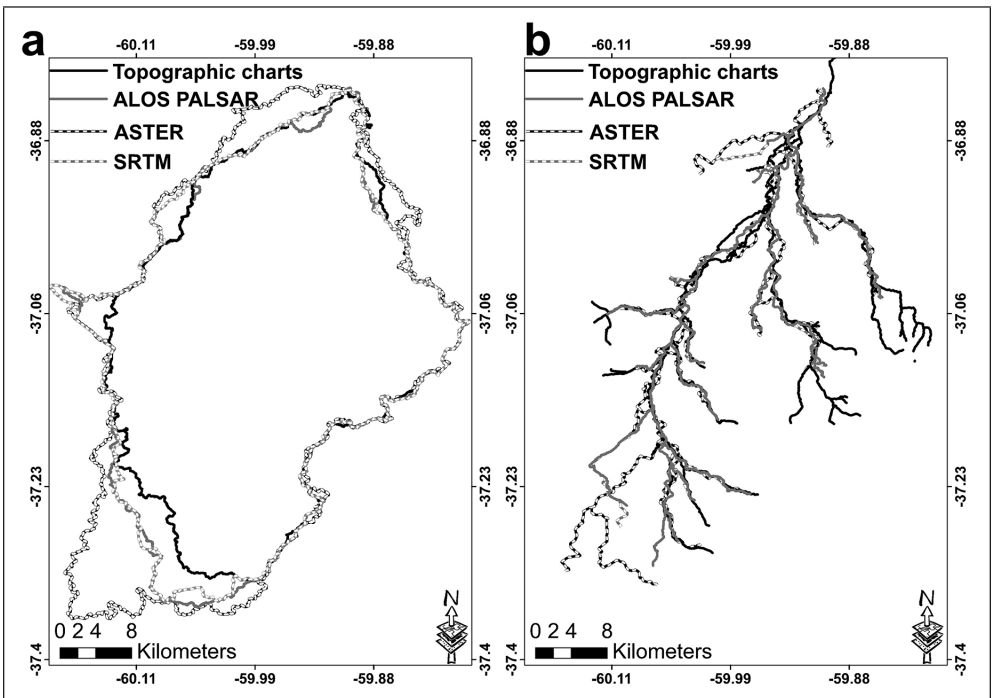

Figure 9. (a) Basin delimitation, (b) Drainage network, for Del Azul upper creek basin obtained from different. Sources: topographic charts, ASTER, SRTM and ALOS PALSAR.

Interpolation Methods

When analyzing the previous results, the models that better represented the topography of the study area were SRTM and ALOS PALSAR. From these two, SRTM was the best at representing the topography in flat areas with a lower density of sampling points. Hence, this was the selected DEM for the analysis of the different interpolation methods. The raw SRTM model in raster format was transformed into its equivalent vector format by means of points, (one point every 30 m). These points were resampled using the different interpolators in order to improve the accuracy of the DEM in the plain zone.

Table 1. Differences between areas of the basin delimited by different means.

Source	Area of the Basin (km²)	Drainage Length (km)	Drainage Density (km/km²)
ASTER	1213	252	4.81
SRTM	1050	214	4.9
ALOS PALSAR	1046	220	4.75
Topographic charts	982	312	3.2

We evaluated the efficiency of five interpolators (i.e., inverse distance weighting, natural neighbor, spline, kriging and ANUDEM). The sensitivity of the terrain to various interpolators was also analyzed in relation to the slope and elevation bands in the study area. The accuracy of the generated model of terrain depends on the interpolation mechanism adopted, and therefore it is necessary to investigate the comparative performance of the different methodological approaches.

The method of interpolation that showed more discrepancies in representing the terrain topography (elevation and slope) was the spline method with an error of ±2.72–4.61 m. The interpolation methods that better represented the elevation bands in the study area (Figure 11a) were, in decreasing order, the inverse distance weighting (RMSE: ±1.7–3.2 m), the ANUDEM (RMSE: ±2–3.3 m) and natural neighbor (RMSE: ±1.8–3.4 m). The kriging method showed a ±2.7–3.9 m RMSE.

Figure 11b shows that the interpolation methods that better represented the slope in the study area were the following, in order of importance: inverse distance weighting (RMSE: ±1.5–3.1 m), ANUDEM and natural neighbor (RMSE: ±1.6–3.2 m for both) and the kriging method (RMSE: ±2.2–3.9 m).

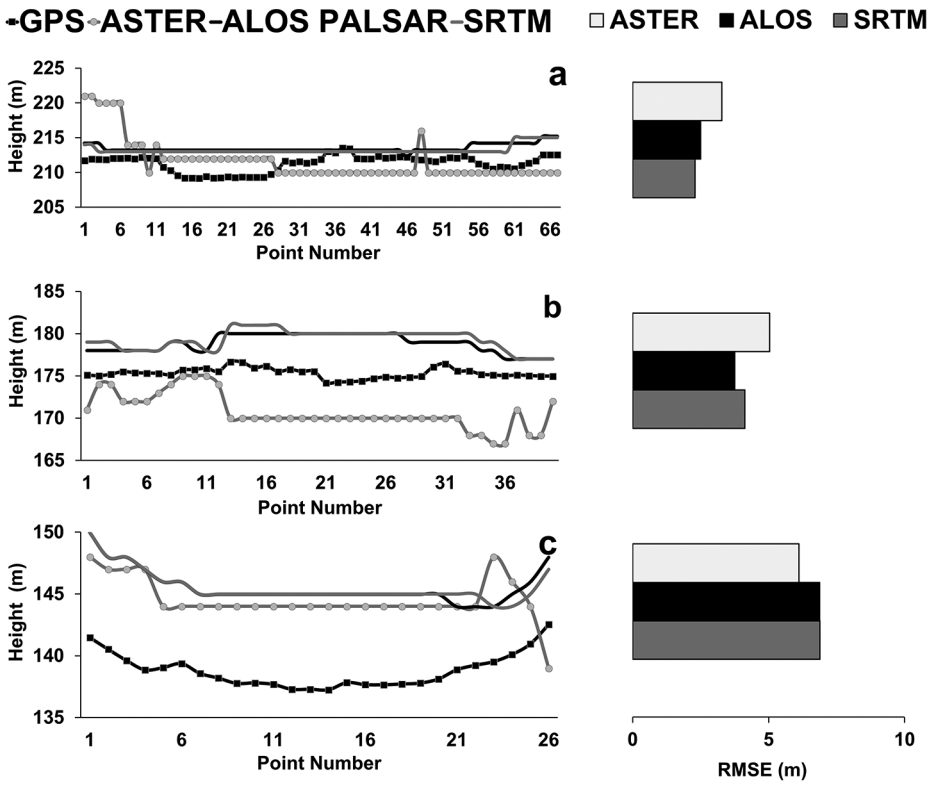

Figure 10. Profile comparison between GPS height measurements and heights obtained from DEMs (ASTER, SRTM and ALOS PALSAR) at the same location point: (a) High zone channel, (b) Middle zone channel, (c) Low zone channel.

Discussion

Our study contributes to improving the information provided by DEMs for plain areas and presents an appropriate methodology for increasing height accuracy and for evaluating the effect of the uncertainties in the currently available models. We evaluated the performance of these models to predict in a realistic way the topography, surface area, slope and flow processes in terms of direction and accumulation, so that they become suitable for use in hydrological modeling. This is to satisfy the need of accurate information for water balance due to it is very sensitive to the topographic attributes, geomorphological and civil structures present in the study area.

Regarding height accuracy, the radar models (i.e., SRTM and ALOS PALSAR) represented more accurately the topography in plain areas. This is because the sensors with which these models work are more accurate than the one for ASTER, capturing with more detail the Earth's surface (De Oliveira and Paradella 2008; Frey and Paul 2012; Frey *et al.* 2012; De Oliveira and De Fátima 2012; Rossetti 2012; Eric *et al.* 2014; Rexer and Hirt 2014; Tan *et al.* 2015; Jarihani *et al.* 2015; Das *et al.* 2015).

One of the drawbacks of DEMs use in plain zones is the poor representation of channels, civil structures and geomorphology. This is because there are <1 m differences in land height and even this difference is small, it plays a significant role in the movement of surface and subsurface water in this type of areas. The SRTM and the ALOS PALSAR were the DEMs that better represented the topography of the study area, unlike ASTER, which showed serious inconsistencies at representing the geomorphology and civil structures. Indeed, Eric *et al.* (2014) stated that the ASTER model had problems in delineating morphological units.

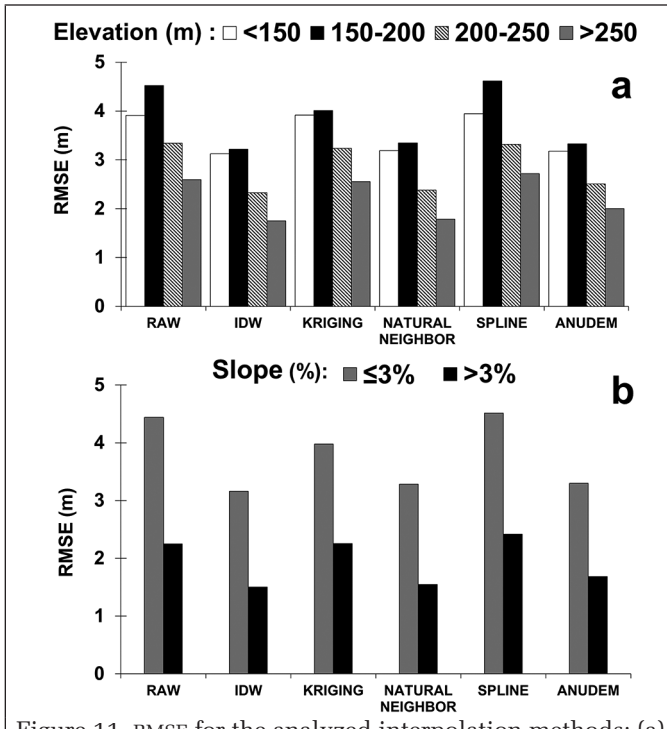

Figure 11. RMSE for the analyzed interpolation methods: (a) elevation bands, (b) slopes.

Regarding the behavior of the interpolators, we found out that these were sensitive to the attributes of the terrain. The inverse distance weighting method demonstrated the best accuracy compared to the other interpolation methods. The generated DEM for the study area based on the SRTM with IDW interpolated data showed a 33% error reduction using, the ANUDEM method, a 27% reduction using the natural neighbor method and a 10% reduction using the kriging method whereas the spline method increased the error by 4% compared to the raw SRTM DEM.

Our study suggests that the most suitable interpolation methods to adequate DEMs for use in plain zones are the inverse distance weighting and ANUDEM. This statement agrees with other published studies such as Aguilar *et al.* (2005), Reuter *et al.* (2007), Paredes *et al.* (2007) and Guo *et al.* (2010).

Our findings showed that topographic variability significantly influences DEMs accuracy and the degree of detail they provide. However, future research is needed to further explore the kriging interpolation method, the semivariogram analysis and the effect of the sampling density, all of which could improve the representation of topographic variability and increase the vertical accuracy.

Regarding the representation of the flow direction and water accumulation, in plain zones, the SRTM model generated a more realistic drainage network latter translated into a better delineated basin (as compared with the basin boundaries obtained using the topographic chart). If we use this product for hydrological modeling it is important to bear in mind that the choice and correction of the DEM will influence the calculation of surface runoff and the flood response time. According to Thomas and Prasanna Kumar (2015) and Dass and Pardeshi (2018), a photogrammetric DEM such as ASTER has inconsistencies in the representation of the drainage networks.

The needs of having readily available elevation data at a detailed scale, affordable and easy to use, has stimulated the development of several satellite platforms designed to generate this type of Earth's surface information. However, although precision ranges are generally well described for each platform, various authors recommend that DEM validations should be performed locally to arrive to more accurate results in order to take better decisions.

Our purpose with this study is to provide DEM users with a set of tools to analyze and evaluate the sensitivity and the uncertainties associated using different topographic parameters.

Conclusions

As seen through this paper, DEMs accuracy to represent terrain morphology, geomorphology and the presence of civil structures in plain areas differ among models. The selection of which DEM to use will have great influence on the modeled water flow patterns. From the three tested DEMs, the SRTM and the ALOS PALSAR were the ones that best represented these topographic variations, with error values of 4.4 m for both. In contrast, the ASTER model presented inconsistencies in delimiting landscape units, with error values above 8 m.

The SRTM and the ALOS PALSAR DEMs showed a better performance in the representation of the morphology for the plain area of the basin whereas the ASTER DEM overestimated the low-stream-order-drainage network and thus provided an inaccurate delimitation of the basin. Therefore, special attention should be taken when choosing the particular DEM for hydrological modeling in plain areas since this choice will surely influence the response time and amount of water moving over the surface.

When analyzing and visualizing the vertical error distribution in plain zones, the spline method is not recommended for elevation data interpolation since this method showed the lowest statistical precision among the analyzed methods. The IDW and ANUDEM methods increased the accuracy of the model in approximately 33% from a raw SRTM (RMSE: ±4.44 m and ±3.2 m for the non-corrected and corrected models, respectively).

Summarizing, when hydrological studies are carried out in plain zones, it is necessary to know beforehand that the SRTM, the ALOS PALSAR and the ASTER DEMs do not correctly reflect the water flow patterns. The associated errors must be corrected by adjusting the heights in the models with the aid of validated information sources such as topographical charts, satellite images, interpolations and vectors based on measurements performed in the field with differential GPS, particularly in roads, channels and depressions. All these considerations should at least be taken into account in order to improve the accuracy of the DEMs for use in plain areas.

Acknowledgments

The authors would like thank the Instituto de Hidrología de Llanuras, Dr. Eduardo Usunoff (IHLLA) and the Consejo Nacional de Investigaciones Científicas y Técnicas (CONICET) for funding this study.

References

Abrams, M. and S. Hook. 2002. ASTER User Handbook Version 2. Jet Propulsion, 1–135.

Abrams, M., H. Tsu, G. Hulley, K. Iwao, D. Pieri, T. Cudahy, and J. Kargel. 2015. The Advanced Spaceborne Thermal Emission and Reflection Radiometer (ASTER) after fifteen years: Review of global products. *International Journal of Applied Earth Observation and Geoinformation* 38: 292–301.

Aguilar, F. J., F. Agüera, M. a. Aguilar and F. Carvajal. 2005. Effects of terrain morphology, sampling density, and interpolation methods on grid DEM accuracy. *Photogrammetric Engineering Remote Sensing* 71 (7): 805–816.

Arun, P. V. 2013. A comparative analysis of different DEM interpolation methods. *The Egyptian Journal of Remote Sensing and Space Science* 16 (2): 133–139.

Barnes, R., C. Lehman and D. Mulla, 2014. An efficient assignment of drainage direction over flat surfaces in raster digital elevation models. *Computers Geosciences* 62:128–135.

Bartier, P. M. and C. P. Keller. 1996. Multivariate interpolation to incorporate thematic surface data using inverse distance weighting (IDW). *Computers Geosciences* 22 (7): 795–799.

Callow, J. N., K. P. Van Niel and G. S. Boggs. 2007. How does modifying a DEM to reflect known hydrology affect subsequent terrain analysis? *Journal of Hydrology* 332 (1–2):30–39.

Carrascal Leal, C. C., G. A. Denegri and M. I. Delgado. 2013. Costos mínimos de compensación y cuantificación de la oferta hídrica en la cuenca alta del río Sauce Grande, Argentina. *Investigaciones Geográficas* 0 (80):55–70.

Chaubey, I., A. S. Cotter, T. A. Costello and T. S. Soerens. 2005. Effect of DEM data resolution on SWAT output. 628:621–628.

Chen, Y., J. P. Wilson, Q. Zhu and Q. Zhou. (2012). Comparison of drainage-constrained methods for DEM generalization. *Computers Geosciences* 48:41–49.

Childs, B. C. 2004. Interpolation surfaces in ArcGIS spatial analyst. *ArcUser*, July–September 2004: 32–35.

Chu, T. and K. E. Lindenschmidt. 2017. Comparison and validation of digital elevation models derived from InSAR for a flat inland delta in the high latitudes of Northern Canada. *Canadian Journal of Remote Sensing* 43 (2):109–123.

Das, A., R. Agrawal and S. Mohan. 2015. Topographic correction of ALOS-PALSAR images using InSAR-derived DEM. *Geocarto International* 30 (2):145–153.

Das, S. and S. D. Pardeshi. 2018. Comparative analysis of lineaments extracted from Cartosat, SRTM and ASTER DEM: A study based on four watersheds in Konkan region, India. *Spatial Information Research* 26 (1):47-57.

De Oliveira Andrades Filho, C. and D. De FáTima Rossetti. 2012. Effectiveness of SRTM and ALOS-PALSAR data for identifying morphostructural lineaments in northeastern Brazil. *International Journal of Remote Sensing* 33 (4):1058–1077.

De Oliveira, C. G. and W. R. Paradella. 2008. An assessment of the altimetric information derived from spaceborne SAR (RADARSAT-1, SRTM3) and optical (ASTER) data for cartographic application in the Amazon region. *Sensors* 8 (6):3819–3829.

Easton, Z. M., D. R. Fuka, M. T. Walter, D. M. Cowan, E. M. Schneiderman and T. S. Steenhuis. 2008. Re-conceptualizing the soil and water assessment tool (SWAT) model to predict runoff from variable source areas. *Journal of Hydrology* 348 (3–4):279–291.

Eric, Z., W. Petrus, D. Clercq and A. V. Niekerk. 2014. An evaluation of digital elevation models (DEMs) for delineating land components. *Geoderma*, 213 :312–319.

Frey, H., F. Paul and T. Strozzi. 2012. Compilation of a glacier inventory for the western Himalayas from satellite data: Methods, challenges, and results. *Remote Sensing of Environment*, 124 :832–843.

Gallant, J. C. and T. I. Dowling. 2003. A multiresolution index of valley bottom flatness for mapping depositional areas. *Water Resources Research* 39 (12).

Gao, X., X. Zhao, P. Wu, L. Brocca and B. Zhang. 2016. Effects of large gullies on catchment-scale soil moisture spatial behaviors: A case study on the Loess Plateau of China. *Geoderma* 261:1–10.

Gesch, D. B., J. Muller and T. G. Farr. 2006. The shuttle radar topography mission data validation and applications. *Photogrammetric Engineering Remote Sensing* 72:233–235.

Gichamo, T. Z., I. Popescu, A. Jonoski and D. Solomatine. 2012. River cross-section extraction from the ASTER global DEM for flood modeling. *Environmental Modelling Software* 31:37–46.

Guevara, C. 2015. Una metodología para el manejo integral de extremos hídricos en una cuenca rural en zona de llanura. caso de estudio: cuenca arroyo Santa Catalina, provincia de Buenos Aires. *Tesis de Maestría en Ecohidrología, Universidad Nacional de la Plata*, 143.

Guo, Q., W. Li, H. Yu and O. Alvarez. 2010. Effects of topographic variability and Lidar sampling density on several DEM interpolation methods. *Photogrammetric Engineering Remote Sensing* 76:701–712.

Hidayat, H., A. J. Teuling, B. Vermeulen, M. Taufik, K. Kastner, T. J. Geertsema and A.J.F. Hoitink. 2017. Hydrology of inland tropical lowlands: The Kapuas and Mahakam wetlands. *Hydrology and Earth System Sciences* 21:2579–2594.

Hutchinson, M. F. 1989. A new procedure for gridding elevation and stream line data with automatic removal of spurious pits. *Journal of Hydrology* 106 (3–4):211–232.

Hutchinson, M., T. Xu and J. Stein. 2011. Recent progress in the ANUDEM elevation gridding procedure. *Geomorphometry* 19–22.

Jarihani, A., J. N. Callow, T. R. McVicar, T. G. Van Niel and J. R. Larsen. 2015. Satellite-derived Digital Elevation Model (DEM) selection, preparation and correction for hydrodynamic modelling in large, low-gradient and data-sparse catchments. *Journal of Hydrology* 524:489–506.

Kellndorfer, J., W. Walker, L. Pierce, C. Dobson, J. A. Fites, C. Hunsaker and M. Clutter. 2004. Vegetation height estimation from shuttle radar topography mission and national elevation datasets. *Remote Sensing of Environment* 93 (3):339–358.

Kimura, H. and N. Ito. 2000. ALOS/PALSAR: The Japanese second-generation spaceborne SAR and its applications. In *Proceedings of SPIE*. 4152:110–119.

Lemoine, F. G., S. C. Kenyon, J. K. Factor, R. G. Trimmer, N. K. Pavlis, D. S. Chinn and T. R. Olson. 1998. The development of the NASA GSFC and NIMA joint geopotential model. *Gravity, Geoid and Marine Geodesy* 117:461–469.

Lin, S., C. Jing, N. A. Coles, V. Chaplot and N. J. Moore. 2013. Evaluating DEM source and resolution uncertainties in the Soil and Water Assessment Tool. *Stochastic Environmental Research and Risk Assessment* 27 (1):209-221.

Ludwig, R. and P. Schneider. 2006. Validation of digital elevation models from SRTM X-SAR for applications in hydrologic modeling. *ISPRS Journal of Photogrammetry and Remote Sensing* 60 (5):339–358.

Martz, L. W. and E. Jong. 1988. CATCH: A FORTRAN program for measuring catchment area from digital elevation models. *Computers Geosciences* 14 (5):627–640.

Moore, I. D., R. B. Grayson and R. Ladson. 1991. Digital terrain modeling: A review of hydrological geomorphological and biological applications. hydrological processes. 5 (1):3–30.

Mukherjee, S., P. K. Joshi, S. Mukherjee, A. Ghosh, R. D. Garg and A. Mukhopadhyay. 2013. Evaluation of vertical accuracy of open source Digital Elevation Model (DEM). *International Journal of Applied Earth Observation and Geoinformation*, 21:205–217.

Pachri, H., Y. Mitani, H. Ikemi, I. Djamaluddin and A. Morita. 2013. Development of water management modeling by using GIS in Chirchik River Basin, Uzbekistan. *Procedia Earth and Planetary Science* 6:169–176.

Paredes, C., W. Salinas, X. Becerra and S. Jiménez. 2013. Evaluación y comparación de métodos de interpolación determinísticos y probabilísticos para la generación de modelos digitales de elevación. *Investigaciones Geográficas* 82:118–130.

Pavlis, N. K., S. A. Holmes, S. C. Kenyon and J. K. Factor. 2012. The development and evaluation of the Earth Gravitational Model 2008 (EGM2008). *Journal of Geophysical Research: Solid Earth* 117 (B4):1–38.

Pontes, P. R. M., F. M. Fan, A. S. Fleischmann, R.C.D. de Paiva, D. C. Buarque, V. A. Siqueira and W. Collischonn. 2017. MGB-IPH model for hydrological and hydraulic simulation of large floodplain river systems coupled with open source GIS. *Environmental Modelling Software* 94:1–20.

Rabus, B., M. Eineder, A. Roth and R. Bamler. 2003. The shuttle radar topography mission-a new class of digital elevation models acquired by spaceborne radar. *ISPRS Journal of Photogrammetry and Remote Sensing* 57 (4):241–262.

Reuter, H. I., A. Nelson and A. Jarvis. 2007. An evaluation of void-filling interpolation methods for SRTM data. *International Journal of Geographical Information Science* 21 (9):983–1008.

Rexer, M. and C. Hirt. 2014. Comparison of free high-resolution digital elevation data sets (ASTER GDEM2, SRTM v2.1/v4.1) and validation against accurate heights from the Australian National Gravity Database. *Australian Journal of Earth Sciences* 61 (2):213–226.

Robinson, N., J. Regetz and R. P. Guralnick. 2014. EarthEnv-DEM90: A nearly-global, void-free, multi-scale smoothed, 90m digital elevation model from fused ASTER and SRTM data. *ISPRS Journal of Photogrammetry and Remote Sensing* 87:57–67.

Rosenqvist, A., M. Shimada, N. Ito and M. Watanabe. 2007. ALOS PALSAR: A pathfinder mission for global-scale monitoring of the environment. *IEEE Transactions on Geoscience and Remote Sensing* 45 (11):3307–3316.

Sanders, B. F. 2007. Evaluation of on-line DEMs for flood inundation modeling. *Advances in Water Resources* 30 (8):1831–1843.

Scioli, C. 2009. Modelación del escurrimiento superficial en áreas de llanura: Implementación y calibración de un modelo distribuido de grilla. *Tesis de Maestría en Hidrología en Llanuras, Universidad de Rosario* 117.

Sharma, A. and K. N. Tiwari. 2014. A comparative appraisal of hydrological behavior of SRTM DEM at catchment level. *Journal of Hydrology* 519:1394–1404.

Shortridge, A. and J. Messina. 2011. Spatial structure and landscape associations of SRTM error. *Remote Sensing of Environment* 115 (6):1576–1587.

Sibson, R. 1981. A brief description of natural neighbour interpolation. *Interpreting Multivariate Data* 21–36.

Sun, G., K. Ranson, V. Kharuk and K. Kovacs. 2003. Validation of surface height from shuttle radar topography mission using shuttle laser altimeter. *Remote Sensing of Environment* 88 (4):401–411.

Tachikawa, T., M. Hato, M. Kaku and A. Iwasaki. 2011. Characteristics of ASTER GDEM version 2. Pages 3657–3660 in *Proceedings Geoscience and Remote Sensing Symposium (IGARSS).*

Tan, M. L., D. L. Ficklin, B. Dixon, A. L. Ibrahim, Z. Yusop and V. Chaplot. 2015. Impacts of DEM resolution, source, and resampling technique on SWAT-simulated streamflow. *Applied Geography* 63:357–368.

Tarboton, D. G. 1997. A new method for the determination of flow directions and upslope areas in grid digital elevation models. *Water Resources Research* 33 (2):309-319.

Tarekegn, T. H., A. T. Haile, T. Rientjes, P. Reggiani and D. Alkema. 2010. Assessment of an ASTER-generated DEM for 2D hydrodynamic flood modeling. *International Journal of Applied Earth Observation and Geoinformation* 12 (6):457–465.

Thomas, J. and V. Prasannakumar. 2015. Comparison of basin morphometry derived from topographic maps, ASTER and SRTM DEMs: An example from Kerala, India. *Geocarto International* 30 (3):346–364.

Vaze, J., J. Teng and G. Spencer. 2010. Impact of DEM accuracy and resolution on topographic indices. *Environmental Modelling Software* 25 (10):1086–1098.

Wahba, G. and J. Wendelberger. 1980. Some new mathematical methods for variational objective analysis using splines and cross validation. *Monthly Weather Review*.

Wechsler, S. P. and C. N. Kroll. 2006. Quantifying DEM uncertainty and its effect on topographic parameters. *Photogrammetric Engineering Remote Sensing*, 72 (9):1081–1090.

Wilson, J. P. 2012. Digital terrain modeling. *Geomorphology* 137 (1):107–121.

Wilson, J. P. and J. C. Gallant. 2000. Digital terrain analysis. *Terrain Analysis: Principles and Applications* 6 (12):1–27.

Wurl, J., C. N. Martínez García and M. Á. Imaz Lamadrid. 2014. Caracterización del peligro por inundaciones en el oasis La Purísima, Baja California Sur, México. *Investigaciones Geográficas, Boletín Del Instituto de Geografía* 87:76–87.

Yan, K., A. Tarpanelli, G. Balint, T. Moramarco and G. Baldassarre. 2014. Exploring the Potential of SRTM Topography and Radar Altimetry to Support Flood Propagation Modeling: Danube Case Study. *Journal of Hydrologic Engineering* 20 (2):1–7.

Yang, X. and T. Hodler. 2013. Visual and statistical comparisons of surface modeling techniques for point-based environmental data. *Cartography and Geographic Information Science* 38 (1):20–35.

Zabala, M. E., M. Manzano and L. Vives. 2015. The origin of groundwater composition in the Pampeano Aquifer underlying the Del Azul Creek basin, Argentina. *Science of the Total Environment* 518: 168–188.

Zhang, T., X. Xu and S. Xu. 2015. Method of establishing an underwater digital elevation terrain based on kriging interpolation. *Measurement* 63:287–298.